Engineering Structures 118 (2016) 97–107

Contents lists available at ScienceDirect

Engineering Structures

journal homepage: www.elsevier.com/locate/engstruct

Behaviour of ultra high performance fibre reinforced concrete columns subjected to blast loading

Juechun Xu [a], Chengqing Wu [a,c,*], Hengbo Xiang [d], Yu Su [a,b], Zhong-Xian Li [a], Qin Fang [d], Hong Hao [e], Zhongxian Liu [a], Yadong Zhang [d], Jun Li [a,b]

[a] TCU-UA (Tianjin Chengjian University-University of Adelaide), Joint Research Centre on Disaster Prevention and Mitigation, China
[b] School of Civil, Environmental and Mining Engineering, The University of Adelaide, SA 5005, Australia
[c] Centre for Built Infrastructure Research, Faculty of Engineering, University of Technology Sydney, NSW 2007, Australia
[d] PLA University of Science and Technology, Nanjing, China
[e] Department of Civil Engineering, Curtin University, WA, Australia

ARTICLE INFO

Article history:
Received 30 December 2014
Revised 17 March 2016
Accepted 21 March 2016
Available online 2 April 2016

Keywords:
UHPFRC
Nano additives
Columns
Blasts
Experimental analysis

ABSTRACT

Ultra high performance fibre reinforced concrete (UHPFRC) is a cement-based composite material mixing with reactive powder and steel fibres. It is characterized by its high strength, high ductility and high toughness and such characteristics enable its great potential in protective engineering against extreme loads such as impact or explosion. In the present study, a series of field tests were conducted to investigate the behaviour of UHPFRC columns subjected to blast loading. In total four 0.2 m × 0.2 m × 2.5 m UHPFRC columns were tested under different designed explosions but all at a standoff distance of 1.5 m. Blast tests were also performed on four high strength reinforced concrete (HSRC) columns with the same size and reinforcement as UHPFRC columns to evaluate their behaviour under the same loading conditions. The data collected from each specimen included reflected overpressures, column deflections at centre and near the supports. Three major damage modes, including flexural, shear and concrete spalling failure modes, were observed. The post blast crack patterns, permanent deflections and different levels of damage observations showed that UHPFRC columns performed superior in blast loading resistance as compared with HSRC columns.

1. Introduction

The analysis and design of civilian and military buildings and structures to withstand shock and blast loading has been a subject of extensive studies in the last decade due to the increase of terrorist attacks around the world. There are two main approaches to protect structures against man-made explosive hazards. One approach is to reduce damage by protecting the structures with external claddings (e.g., aluminium foam); the other is to strengthen the structures to better withstand explosion-induced loads such as by applying ultra-high performance fibre reinforced concrete (UHPFRC) [1]. Based on standoff distance and charge weight of detonations, blast loads can be categorised into contact, close-in and far field detonation. Contact detonation is a case that explosive is in contact with a structure, therefore, contact blast load is a high-intensity and non-uniform. For close-in detonation, it is a spherical shock wave generated by the explosion striking a structure with a non-uniform and impulse-dominated load. Far field detonation is the explosive located at a large distance from the structure, where a planar wave with a uniform load is applied to the structures. The main aim of the present research is to investigate the capabilities and dynamic response of ultra-high performance fibre reinforced concrete columns against close-in blasts.

UHPFRC members are investigated in the current study because of their outstanding safety, serviceability, durability and ductility [2–5]. Ultra-high performance concrete is known as a reactive powder concrete that can provide compressive strength up to 200 MPa and flexural tensile strength up to 40 MPa while exhibiting strain-hardening behaviour under uni-axial tension [6,7]. There are two important considerations in selecting UHPFRC columns to resist blast loading, i.e., their capability of preventing catastrophic failure like progressive collapse and reducing fragmentation due to projectiles [8]. Basically, the most significant characteristics of UHPFRC are its high compressive/tensile strength and outstanding ductility stemming from inclusion of steel fibre, which lead to a

* Corresponding author at: Centre for Built Infrastructure Research, Faculty of Engineering, University of Technology Sydney, NSW 2007, Australia. Tel.: +61 2 9514 2742.
E-mail address: chengqing.wu@uts.edu.au (C. Wu).

http://dx.doi.org/10.1016/j.engstruct.2016.03.048
0141-0296/

dramatic increase of the energy absorption capacity of UHPFRC members and prevent them from suffering catastrophic failure under blast loads. Also, the recent development in nano-material science has been included to further improve the strength and energy absorption capacity of UHPFRC members so that their sizes can be reduced significantly in comparison with use of conventional concrete counterparts, leading to a remarkable reduction of material used in structural members with a much lower carbon footprint and sustained more active load on members before and after blast events [8]. Furthermore, as mentioned by Brandt [9], steel fibres create a homogeneous matrix in the mix and bridge the gaps of the micro-crack so as to control local crack opening and propagation as well. Thus in addition to increasing integrity of a structure, it is envisaged that application of UHPFRC will contribute to reducing spalling and scabbing.

In recent years there have been considerable numerical and experimental work conducted to understand UHPFRC material under both static and dynamic loading condition [10–18]. However, because of the high technical requirements, high costs of manufacturing UHPFRC and the security restrictions required for full scale blast tests, experimental studies on UHPFRC members against blasts are very limited. The results of 72 fibrous-reinforced concrete slabs against explosive loading tests were presented by Williamson [19] and it was reported that there is only slight difference in response of high-strength and medium-strength concrete, when used in conjunction with fibres under explosive loading. The experimental data revealed that the failure mode was primarily flexure for a slab in a vertical position with bearing only on two sides, also, the concrete mixed with steel or nylon fibres could be significantly reinforced to withstand the stresses, and effectively reduce the amount and velocity of fragments. Some experimental investigations have been conducted to examine the blast resistant capability of concrete panels/beams/slabs made of UHPFRC materials [7,20–22]. Compared with structures made of normal concrete, these tests not only verified that UHPFRC members could perform extremely well, surviving with minor cracks under the applied blast loads, but also proved that UHPFRC structure could minimize the risk of injury or damage caused by concrete debris as they did not break into fragments.

The study [23] on UHPFRC structures subjected to high strain rates has revealed some important differences on behaviours of UHPFRC subjected to relatively low strain rate dynamic loads. In the latter study, for determining the plates subjected to quasi-static loading, three- and four-point bending tests were applied and drop weight tests were performed in order to apply dynamic three-point-bending loading to UHPFRC plates [23]. Wu et al. [24] conducted a series of blast tests on evaluating the effectiveness of slabs using different materials as blast enhancement reinforcement, and some slabs retrofitted with fibre reinforced polymer plates, others constructed with ultra-high performance concrete. It was reported that the reinforced ultra-high performance fibre concrete slabs which suffered least damage was superior to all slabs made of other concrete materials, confirming that ultra-high performance fibre concrete (UHPC) is a more effective material for use in structures susceptible to terrorist attack or accidental impacts. These studies have generally indicated the benefits of UHPC in improving damage tolerance, enhancing control of cracking and spalling, and the ability to minimize the flying debris from damaged slabs and beams. However, most of the information and results provided by the studies have been used for evaluating the application of UHPC on slabs/beams and there is little published literature pertaining to resistance and behaviour of UHPC columns under blast loading.

Several researchers have studied the blast vulnerability of RC columns with/without FRP-retrofitted composites using blast experiments, numerical prediction and drop-weight tests; and different failure modes have been observed [25–28]. For analysing columns under blasts, a general classification of different failure modes needs to be established according to orientations of major cracks. Three failure modes are generally characterized. In general, flexural response governs failure mechanism when plastic hinges form in centre and supports of columns. If the static shear-bending capacity ratio is less than unity or under high-velocity impact or blast loading, some columns may collapse in a shear failure mode due to development and widening of severe diagonal cracks and rupture of longitudinal rebars [29–32]. Furthermore, as the current research is dealing with a close-in blast loading condition, the extremely high intensity and short duration of blasts give rise to localized failure modes such as direct shear failure mode, spalling and scabbing which are under less consideration in the previous literatures.

The objective of this study is to experimentally investigate whether UHPFRC columns can effectively improve their resistance to blast loads at relatively close standoff distance. In total, 8 column specimens, including 4 specimens built with UHPFRC, and 4 specimens built with HSRC were tested under blast loads ranging from 1 kg to 35 kg equivalent TNT at a distance of 1.5 m. The experiment program including constructing specimens, test set-up and procedure is described. Particular interests of assessing the nature of damage and dynamic response, overpressure, duration time, displacement and failure modes are well-documented and analysed. The concluding remarks are presented in the final section.

2. Outline of experiment

2.1. Material characteristics

In the current UHPFRC material composition, constant water to binder ratio 0.16 is adopted. Aggregates (river sand) at the same weight dosages (40% by weight) was used, a constant content of silica fume, silica flour was used to provide high pozzolanic effect that accelerated the hydration process and enhanced the material compressive strength. To further improve the performance of matrix, nanoscale $CaCO_3$ particles which acted as an effective filling material and also provided high pozzolanic reactivity had been used. The nanoparticle Nano-$CaCO_3$ has mean particle sizes about 40 nm and the specific surface area (in BET methods) more than 30 m^2/g.

Micro steel fibre (MF) was added into the mixtures and MF has 0.1 mm diameter and 6 mm length which can sustain tensile strength more than 4000 MPa. The steel fibres at a dosage 2.5% by volume were used. This dosage was decided on the basis of a series of preliminary tests. Table 1 shows mix proportions of UHPFRC/HSRC. Please note that HSRC has the same proportions of mix design as UHPFRC except fibre material addition.

Static test results based on uniaxial compression and four-points bending tests indicated that the specified UHPFRC compressive strength and flexural tensile strength at 28 days was 148 MPa and 32 MPa, respectively.

2.2. Specimen geometry

The test specimens consist of four UHPFRC columns (that is, U1A, U1B, U2A and U2B) with span length 2.5 m, having square cross section of 0.2 m. The geometry of UHPFRC column, layout of longitudinal reinforcements and spacing of transverse reinforcement are shown in Fig. 1. The reinforcing bar has diameter of 16 mm with cross-section area of 201.1 mm^2 and the centre-to-centre spacing of 57 mm. The thickness of the concrete cover is 35 mm; the yield stress and ultimate strength of high strength reinforcing bars are 1450 MPa and 1600 MPa, respectively.

Table 1
Composition of UHPFRC/HSRC.

Constituent	Cement (kg)	Silica fume (kg)	River sand (kg)	Glenium (L)	Water (kg)	Water/binder (%)	Steel fibre (%)	Nano $CaCO_3$ (%)
1 m^3 mixture	995	229	1051	60	197	16	2.5	3

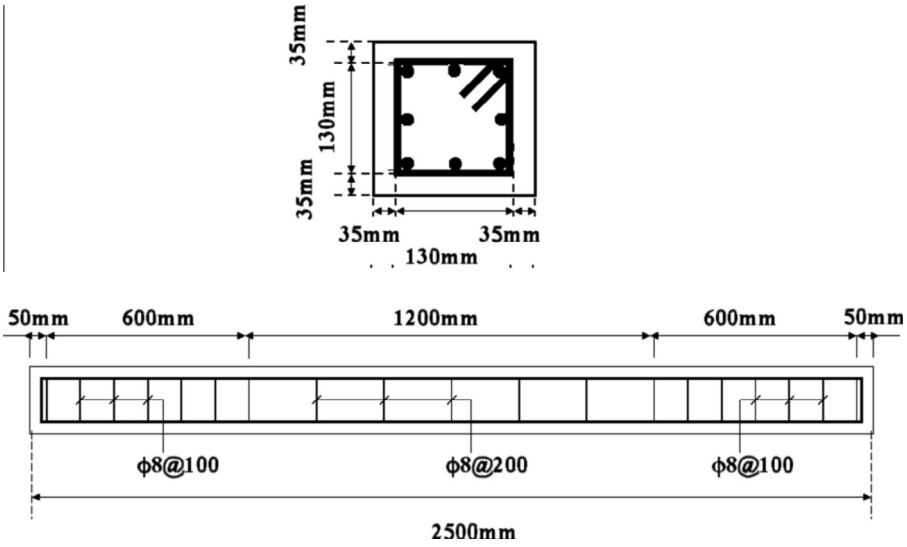

Fig. 1. Geometry of the UHPFRC and HSRC specimen.

The columns were divided into two groups, with specimens in each group being nominally identical. The columns in Group U were produced by using UHPFRC and Group H by HSRC. The charge weights, scaled distance, specimen geometry for the experimental program are provided in Table 2. It should be noted that U1A was subjected to two shots, that is, 1 kg TNT blast loading followed by 35 kg TNT charge loading (so was U2A), while U1B was subjected to 17.5 kg TNT blast loading. Such arrangement was designed to observe different response modes and possible damages of column. 1 kg blast loading was designed for elastic response, 17.5 kg blast loading was designed for plastic response while 35 kg blast loading was designed for possible failure.

2.3. Experimental set-up

A schematic diagram of the test instrumentation is shown in Fig. 2. The test set up was commenced by placing the specimen in an excavated test pit with its top surface at the same level as ground. This design is selected to eliminate the clearing effect. When preparing the test field, an excavated test pit with dimensions 5 m × 1.7 m × 2 m was dug for containing the specimen and housing the electrical cables and instrumentation equipment. The installation arrangement of UHPFRC columns is shown in Fig. 3.

Steel frame of dimension 2600 mm × 400 mm × 1000 mm as shown in Fig. 4(a) was built with a clamping system to ensure that the test specimens were firmly placed inside the frame and prevented the column from uplifting. There were five box-type structures mounted under the frame for placing the displacement measurement devices. With this design, the wiring connection and LVDT devices were fully protected during the blast tests. After placing the column between the supported frames, the whole frame was lowered into the ground, thus there were only top surface of the column with area 200 mm × 2500 mm exposed to the blast wave. In order to prevent the unreliable experimental results due to the vertical movement at the supports, steel yokes were used, which prevented vertical movement against column rebound, thus making the effective span of the specimen

Table 2
Experimental program.

Column name	Description	Fibre content (%)	Normal force (kN)	Charge distance D (m)	Scaled distance (m/$kg^{1/3}$)	TNT equivalent charge weight (kg)
U1A	UHPFRC	2.5	0	1.5	1.5	1
U1A	UHPFRC	2.5	0	1.5	0.5	35
U1B	UHPFRC	2.5	0	1.5	1.5	1
U1B	UHPFRC	2.5	0	1.5	0.6	17.5
U2A	UHPFRC	2.5	1000	1.5	1.5	1
U2A	UHPFRC	2.5	1000	1.5	0.5	35
U2B	UHPFRC	2.5	1000	1.5	1.5	1
U2B	UHPFRC	2.5	1000	1.5	0.6	17.5
H1A	HSRC	0	0	1.5	1.5	1
H1A	HSRC	0	0	1.5	0.6	17.5
H1B	HSRC	0	0	1.5	1.5	1
H1B	HSRC	0	0	1.5	0.8	8
H2A	HSRC	0	1000	1.5	0.6	17.5
H2B	HSRC	0	1000	1.5	0.8	8

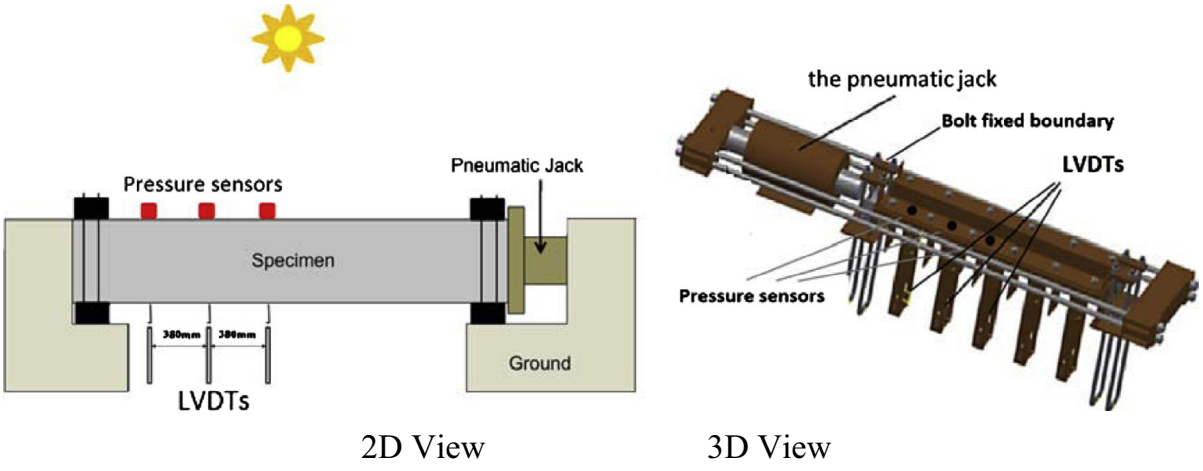

Fig. 2. Schematic diagram of the support condition.

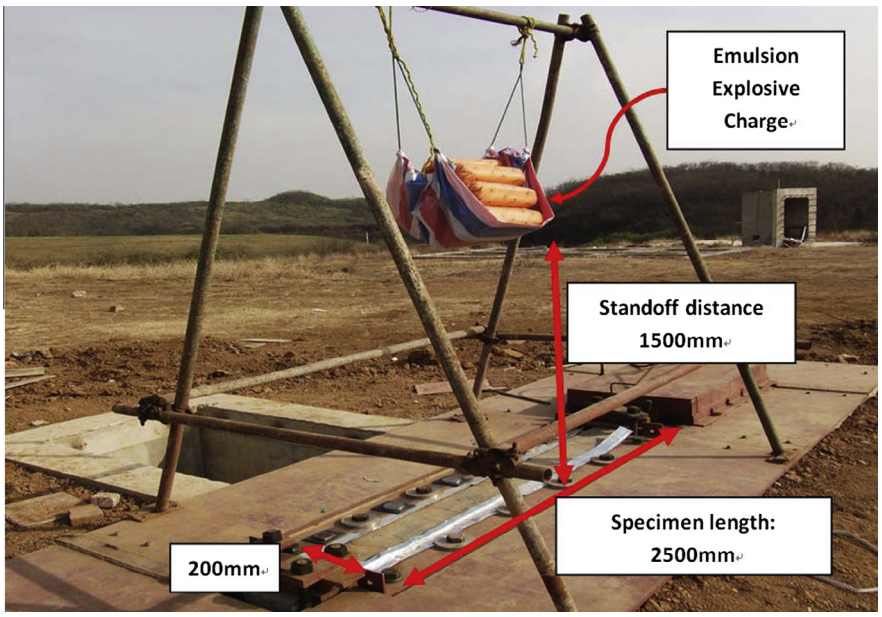

Fig. 3. Experimental set up.

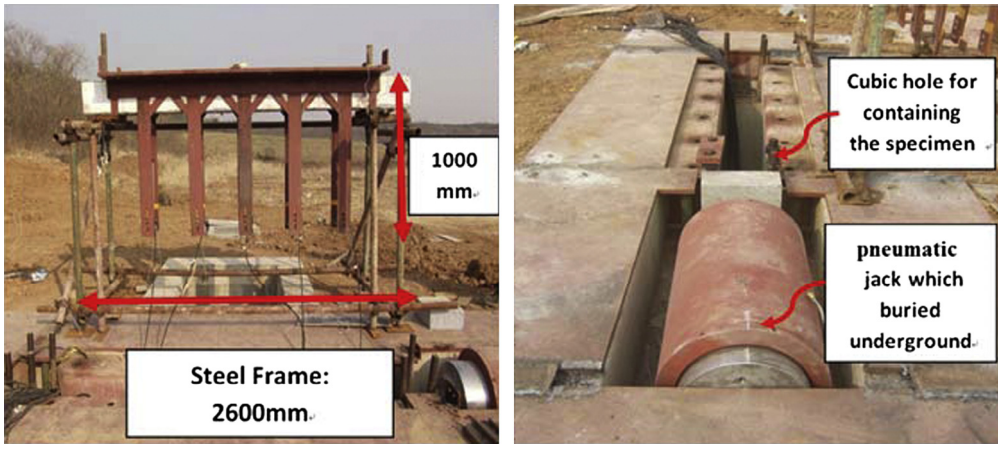

(a) specified steel frame design (b) Pneumatic jack buried underground

Fig. 4. Steel frame and axial loading supply system.

2300 mm. On the other side, the axial loading was applied using a pneumatic jack as shown in Fig. 4(b). In the test, axial loading was applied to some of UHPFRC columns. For typical ground floor column in a low-to-medium rise building, its axial load ratio (service load versus loading capacity) is from 0.2 to 0.4. Considering high mechanical performance of UHPFRC and its comparable density to normal strength concrete, in the current study, an axial load of 1000 kN which equals to approximately 20% their loading capacity was used during the tests and was kept as a constant for all UHPFRC samples. For comparison purpose, HSRC columns C8A and C8B were loaded with the same axial load, i.e. 1000 kN which equals to their 50% loading capacity.

Cylinder emulsion explosive charge weights of 1.4–48 kg were placed at 1.5 m height above the specimen. The nominal TNT equivalence factor for emulsion explosive charge is 1.4.

2.4. Instrumentation

In order to record the column displacement, linear variable differential transducers (LVDT) were placed underneath the column specimens. Fig. 5 shows the locations of LVDTs for each test specimen. With a span length of 2500 mm, there is a LVDT placed at 1/2 (mid-span); others were placed at 1/3rd, and 1/6th distance along the span of the column. The LVDTs have sampling rate of 0.2 MHz and a stroke range of 300 mm. As mentioned above, these LVDTs were installed into a box-like steel frame below the specimens and placed in an excavated test pit to avoid blast induced damage. However, prior to the preliminary close-in blast testing, an unsuccessful attempt was observed in which all the LVDTs were destroyed by the extremely high shock pressure passing through the gap between the specimen and the supporting rig. To better protect the instruments in the following tests, two layers of rubber pad and a thin steel panel were used to cover the gaps between the column and the supporting system. Please note that the additional rubber pads and steel panels did not hinder the free movement of columns.

For measuring the reflected pressures, pressure transducers were installed at the distance of 0 mm, 380 mm and 760 mm away from the centre of the specimen, respectively, as shown in Fig. 6. It should be noted that the pressure measurements depend on the sensitivity of the pressure transducers. The measuring range of the pressure sensors was up to 70 MPa. The signals from the LVDTs

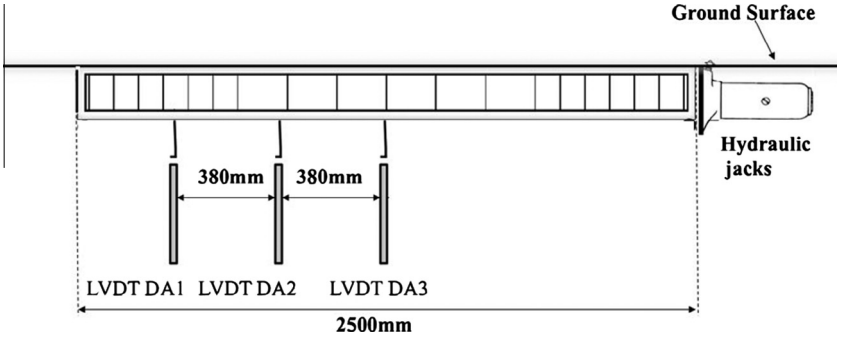

Fig. 5. LVDT locations.

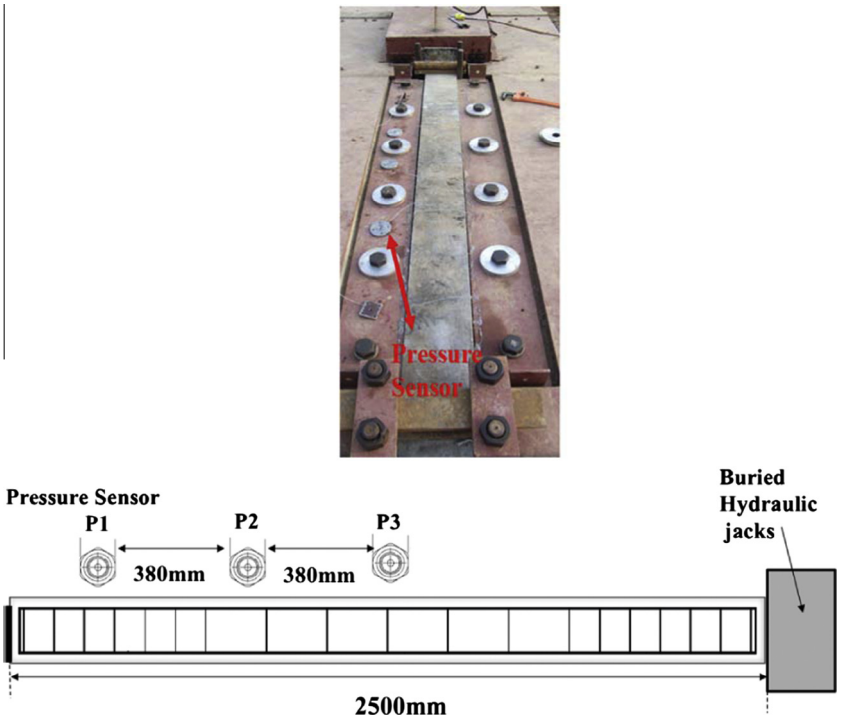

Fig. 6. Pressure sensor locations.

and pressure sensors were transferred and stored by the data acquisition system (DAC) as digital data. The unit had a maximum recording frequency of 0.2 MHz per channel, and five channels for pressure recording and five channels for displacements recording simultaneously during the tests.

2.5. Test procedure

All specimens were tested under combined with/without static axial loading and blast loads; a clear distance between charge centre and centre of specimen is 1.5 m. Each column was tested by the following procedures:

(1) The first step of the experiment was to place the specimen on top of the steel frame, connect all the LVDTs and check connections and functionality.
(2) The whole frame with specimens needed to be placed in a horizontal position and lowered into the testing frame, making sure that the top surface of the column at the same level as the ground surface.
(3) Then make sure the designed steel yokes performed well to let specimen free-standing at two lateral sides of the test position. The other support was connected with the pneumatic jack which located at the same level with the column to make sure that the axial load could be transferred from the pneumatic jack to the column.
(4) Afterwards, the pressure transducers needed to be properly installed and checked.
(5) Explosive was placed using the guided line 1.5 m above the centre of the column.
(6) Finally the detonation was triggered and the test data was recorded.

3. Results and discussion

The data for UHPFRC columns against blast loading were recorded, including: (1) typical pressure–time histories for different charge weights; (2) displacement versus time histories measured by the LVDTs at mid-span and near supports. All data recorded was used to compare the performance of high strength reinforced concrete (HSRC) specimens with UHPFRC columns, so as to better understand the effect of UHPFRC in improving the blast resistant capability. The summaries of the test results for UHPFRC and HSRC columns are listed in Table 3. The table reports the maximum mid-span displacement, and residual deflection for each specimen.

Table 3
Summary of UHPFRC and HSRC series test results.

Specimen	Charge weight (kg)	Axial load (kN)	Maximum deflection (mm)	Permanent deflection (mm)
U1A	1	0	2.0	0
U1A	35	0	–	21
U1B	1	0	2.0	0
U1B	17.5	0	63	18.5
U2A	1	1000	–	0
U2A	35	1000	68	23
U2B	1	1000	1.2	0
U2B	17.5	1000	29.3	4
H1A	1	0	2.4	0
H1A	17.5	0	82.6	2
H1B	1	0	2.6	0
H1B	8	0	46.9	1
H2A	17.5	1000	56.0	12
H2B	8	1000	38.0	7.5

3.1. Blast pressure measurements

The applied blast loads resulted from four charge weights which are 1 kg, 8 kg, 17.5 kg and 35 kg TNT equivalence at different scale distances were captured by the three pressure sensors located in different places as indicated in Fig. 7. Empirical perdition on the peak blast overpressure and duration is based on UFC 3-340-2. According to the comparison between experimental and empirical blast pressure time histories as shown Fig. 7, it is generally concluded that empirical method can give reasonable overpressure decay prediction although it underestimates the peak blast overpressure for all the blast scenarios. However, the deviation between the experimental and empirical predictions is relatively small.

As expected, the greater charge weight tends to cause larger reflected pressure. In general, it can be observed that the average peak overpressure recorded has a dramatic increase from 1 kg to 8 kg, to 17.5 kg, and finally 35 kg explosive loading. Furthermore, it is worth noting there is always a second peak over-pressure followed the first peak pressure for most of the data collected from different pressure sensors. This could be ascribed to the complicated process of the detonation of the emulsion explosives. Unlike the incidental explosion engendered by integrated TNT charge, several emulsion explosive charges wrapped for achieving the equivalent TNT blast pressure magnitude were accumulated together, resulting in continuous explosion characteristics. The foregoing reflected blast waves were combined with the subsequent ones, creating different applied loading with several peak pressures. Another possible reason is that a lot of sand and soil particles travel along with it, which inevitably hit on the pressure transducer when the blast wave travels toward a test specimen. As the pressure transducer is highly sensitive, the pressure resulted from the particle collision is therefore also regarded as part of the blast load.

3.2. Displacement versus time period of vibration

To assess the effectiveness of UHPFRC columns in enhancing blast resistance, the maximum displacements and permanent deflections measured at the centre of specimens are given in Table 3 and typical displacements for cases U1B and U2B of UHPFRC specimens and H1A, H1B, H2A and H2B of HSRC specimens are used to compare UHPFRC columns with/without axial load and HSRC specimens with/without axial load under similar blast loads plotted in Figs. 8–10. These figures have been classified into three groups based on the charge weights varying from 1 kg to 8 kg, and 17.5 kg.

As mentioned before, LVDTs were placed at three different positions for recording the displacements with the legend of DA1, DA2 and DA3 in Figs. 8–10, DA1–DA3 represented the LVDTs placed at 1/6th 1/3rd and 1/2 (mid-span) of the distance along the column, respectively. Fig. 8(a) and (b) indicates the displacements of UHPFRC specimens U1B and U2B under the 1 kg charge weight load recorded by the LVDTs at three different locations. Generally speaking, the responses from each specimen were very similar; the largest displacement was recorded by DA3 at the centre of the specimen, and the value recorded by DA2 was typically less than the mid-span deflection and finally DA1 located near the support followed a very similar trend but the least deflection to that recorded by DA2 and DA3. The results of specimens U1B and U2B under the 17.5 kg charge weight loads as shown in Fig. 8(c) and (d) demonstrate similar phenomena. As expected, larger charge weight (17.5 kg charge weight) yields larger deflection. Fig. 9 shows the displacements of HSRC specimens H1B and H2B under the 8 kg charge weight load recorded by the LVDTs at two different locations (DA2 and DA3). Similar phenomenon is observed again.

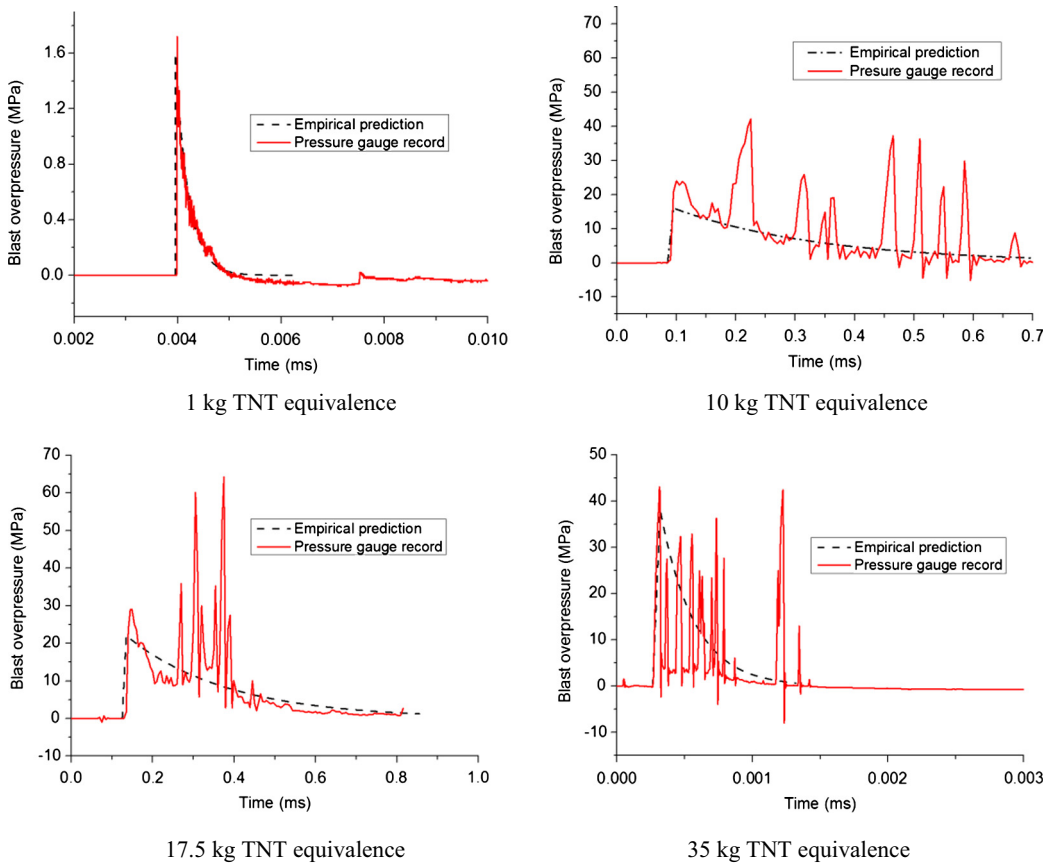

Fig. 7. Blast pressure time-histories.

The effect of axial load was investigated by applying two different axial loads, namely 0 kN and 1000 kN, on both UHPFRC and HSRC specimens by comparing their displacement–time histories under the same blast loads. As can be shown in Fig. 10(a), for comparing the displacements under the same 1 kg TNT equivalent charge loading, the maximum displacement measured at mid-span of UHPFRC column U1B without axial loading was 2.0 mm, while UHPFRC specimen U2B with 1000 kN axial loading was 1.2 mm. This phenomenon shows that the addition of axial load leads to a reduction of 40% deflection of the UHPFRC specimens. Comparing with the deflection of U1B (64 mm), U2B (29 mm) has approximately 55% reduction of displacement, demonstrating that the axial loading plays significant role on increase of the blast resistance capacity. The similar phenomenon was observed when comparing HSRC specimens H1A without axial loading (mid-span displacement is 82.6 mm) with H2A with 1000 kN axial load (mid-span displacement is 56.0 mm) as shown in Fig. 10(b). Furthermore, a comparison between HSRC specimens H1B (mid-span displacement is 46.9 mm) and H2B (mid-span displacement is 38.0 mm), in which both specimens were subjected to 8 kg charge weight loading as shown in Fig. 9, indicated the significant reduction of displacements that can be attributed to addition of the axial loading. This is because the axial load applied on the column increases the moment capacity and its nominal shear strength of the column. The axial loading also changes the column boundary condition by limiting the end rotation and introducing possible compressive membrane effect, the influence from boundary change outweighs the P-delta effect which results in a reduced mid span deflection. However, it should be notated that as columns experience large deflection and plastic hinges formation occurs at mid-span and fixed ends, axial loads will amplify the displacement and internal moment due to the P–Δ effect.

The results in Fig. 10 also indicated that the addition of steel fibre in columns (U1B and U2B) substantially reduced the mid-span displacements when compared to a high strength reinforced concrete columns without inclusion of steel fibre (H1A and H2A). With addition of steel fibre, there is a 23% reduction of deflection for U1B (63 mm) when comparing to H1A (82.6 mm) under the same 17.5 kg blast load. Also when comparing U2B with H2A under the same 17.5 kg blast load with 1000 kN axial loading, column U2B has a maximum mid-span deflection which is approximately 47% smaller than HSRC column H2A. Similar reduction of deflection is also observed for U1B (2.0 mm) in comparison with H1A (2.4 mm) under the same 1 kg blast load with 1000 kN axial loading. The above results are expected since UHPFRC has drastically greater compressive and tensile strengths, as well as ductility due to high steel fibre contents [7].

3.3. Crack profiles and failure modes

The effectiveness of steel fibres is also determined by comparing the post-blast crack patterns of UHPFRC specimens to those of HSRC columns. Detailed descriptions of typical crack profile together with classification of the failure modes are presented in this study. Generally speaking, four levels of damage have been characterized to describe the post-blast specimens, which are light, moderate, heavy and severe.

For light damage, column is in good service condition with almost no lateral deflection, only hairline cracks can be observed. When moderate damage occurs, formation of cracks can be found

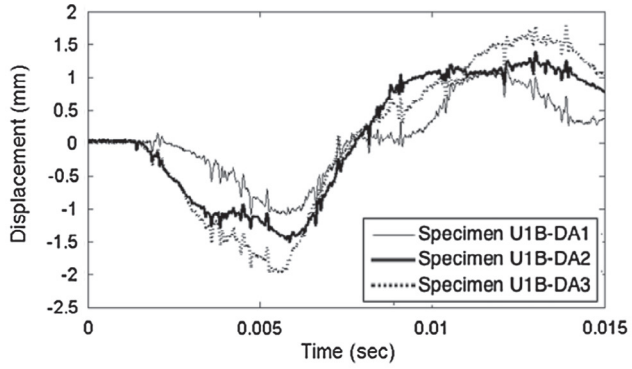

(a 1kg)

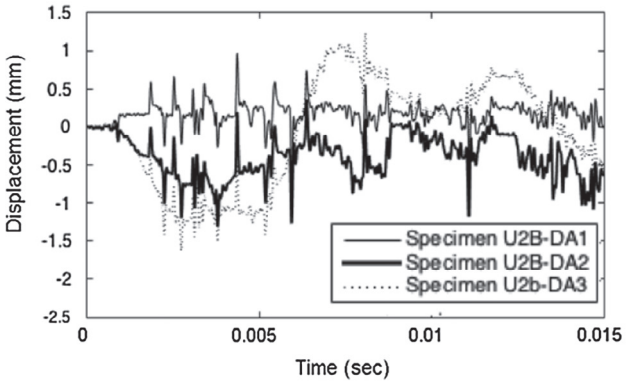

(b 1kg)

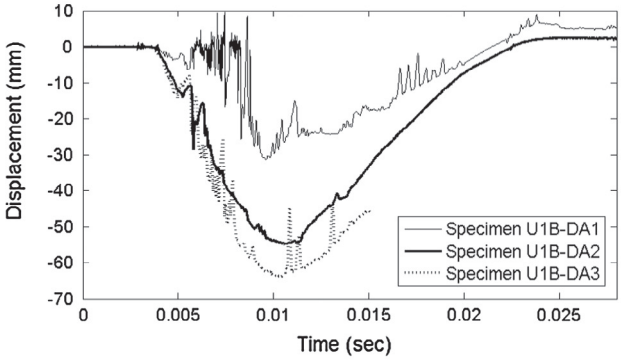

(c 17.5kg)

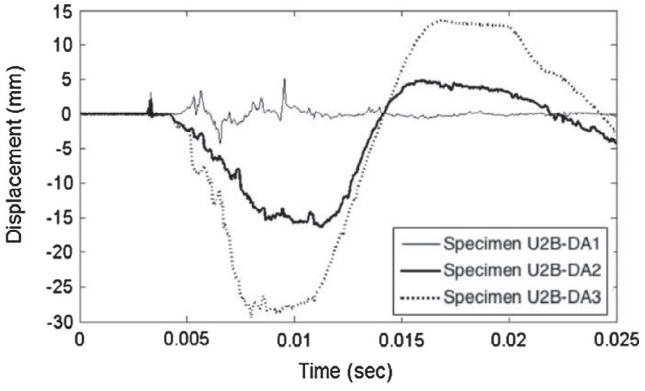

(d) 17.5kg

Fig. 8. Displacement time profiles of UHPFRC specimens under different charge weight loads.

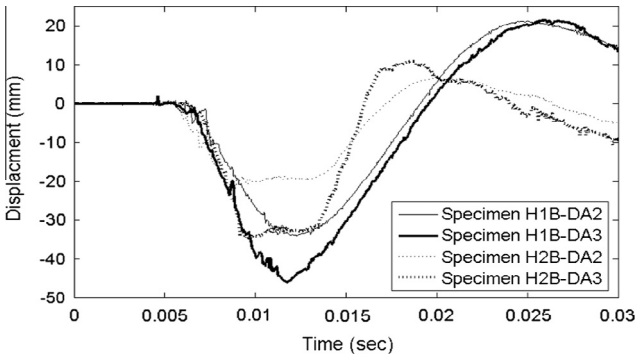

Fig. 9. Displacement time profiles of HSRC specimens under the 8 kg charge weight loads.

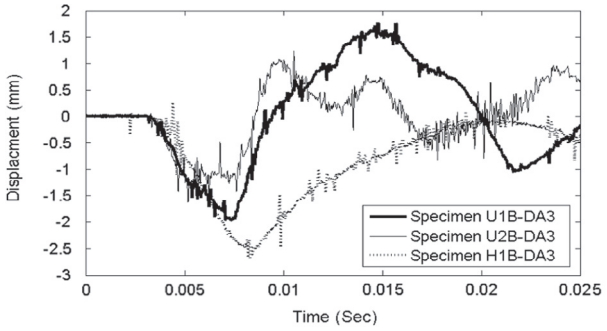

(a) 1kg

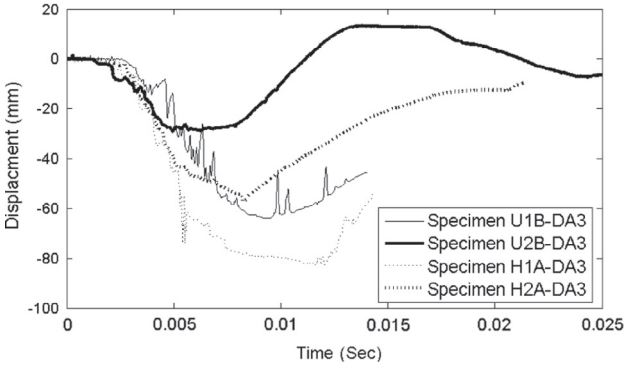

(b) 17.5kg

Fig. 10. Effects of axial loads on displacement time profiles of specimens.

at the distal face and the crack width cannot exceed 5 mm. Following that, heavy damage is defined when concrete crushing at proximal surface is observed together with massive cracking of concrete at distal surface; the crack width is more than 5 mm. The summary of the maximum deflection, level of damage and failure modes is given in Table 4. The post damage photographs of UHPFRC and HSRC specimens under different blast loadings can be observed in Figs. 11 and 12, respectively.

Generally, it is seen in Table 4 that UHPFRC columns in an average sense suffered much less damage than HSRC columns. Based on the post blast observed damage scenarios, most of UHPFRC specimens are in light or moderate damage level, however, HSRC specimens suffered heavy to severe damage under similar or smaller

Table 4
Post-blast damage analysis.

Specimen	Charge weight (kg)	Axial load (kN)	Post-blast failure mode description	Post-blast observed damage level
U1A	35	0	Flexural	Moderate
U1B	17.5	0	Flexural	Moderate
U2A	35	1000	Flexural	Moderate
U2B	17.5	1000	Flexural	Moderate
H1A	17.5	0	Brittle shear failure near supports combined with flexural failure and massive concrete spalling	Severe
H1B	8	0	Brittle shear failure near supports combined with flexural failure and massive concrete spalling	Heavy
H2A	17.5	1000	Brittle shear failure near supports combined with flexural failure and massive concrete spalling	Severe
H2B	8	1000	Brittle shear failure near supports combined with flexural failure and massive concrete spalling	Severe

blast loading. As shown in Figs. 11 and 12, the response mode of UHPFRC columns is shown to be primarily flexural while HSRC columns tend to fail under shear with fragments scattered extensively.

The influence of axial loading on the damage of the specimens was also under investigation. The results on columns tested with axial loading ranging from 0 to 1000 kN showed that axial loading can affect the post damage scenario. When observing the post damage scenario of HSRC columns in Fig. 12, columns with axial loading exhibit more severe damage in comparison to the specimens without axial loading. For example, for specimen H1B without axial loading, typical thin cracks with limited spalling of concrete from the surfaces of the column was observed, although the diagonal splitting width of H1B was 2 mm and the crushing width was 300 mm, the column remains intact. In contrast, there are several diagonal slitting developed from the bottom of the specimen H2B (with 1000 kN axial load) and extend to the top of the column, and also massive crushing of compression concrete was observed; the large diagonal crack with 15 mm width tends to disengage the column into different pieces. This situation may be due to the fact that axial compression strain and flexural compression strain from the blast load exceed the ultimate strains of the columns at the supports. Under the combination force of blast and axial loading, the concrete material is under a complex three dimensional stress state, and increasing of axial loading increases the load applied on the concrete element and thus leading to more severe damage. The addition of axial loading may reduce the capacity of the column to withstand blasts as a result of the pre-compressed concrete being close to material failure.

U1A Specimen with 0 axial load under 35 kg charge weight loading

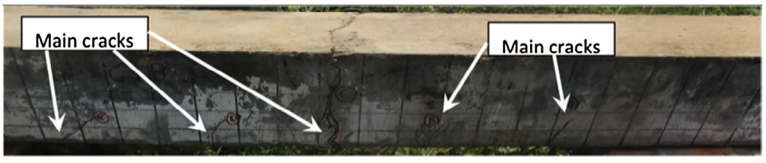

U1B Specimen with 0 axial load under 17.5 kg charge weight loading

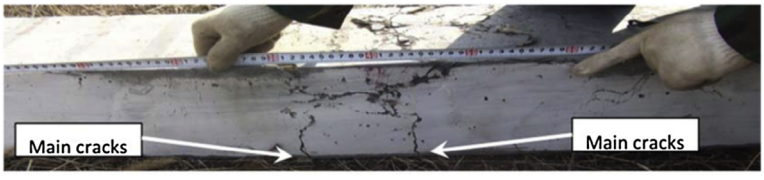

U2A Specimen with 1000 kN axial load under 35 kg charge weight loading

U2B Specimen with 1000 kN axial load under 17.5 kg charge weight loading

Fig. 11. Post blast damage situations of UHPFRC columns.

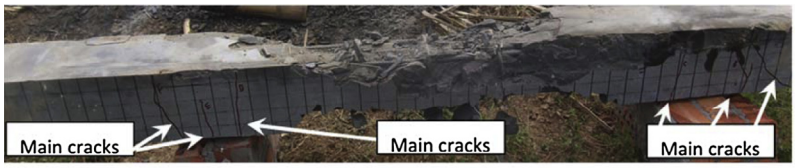

H1A Specimen with 0 axial load under 17.5 kg charge weight loading

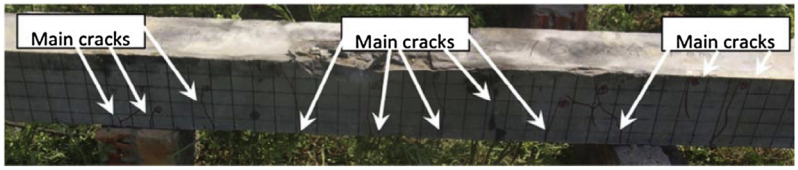

H1B Specimen with 0 axial load under 8 kg charge weight loading

H2A Specimen with 1000 kN axial load under 17.5 kg charge weight loading

H2B Specimen with 1000 kN axial load under 8 kg charge weight loading

Fig. 12. Post blast damage situations of HSRC columns.

4. Conclusion

The experimental results of 8 columns under explosions at different scaled distances are presented in the current study. Evaluation was based upon the capability of UHPFRC columns to resist blast loading; the values obtained from the tests on HSRC specimens were used as the basis of comparison. Based on the data presented herein, the following conclusions are delivered:

1. Comparing the results of HSRC and UHPFRC specimens shows that UHPFRC specimens can effectively resist the overpressures and shock waves resulted from high explosives, reducing the maximum and residual displacements of columns when subjected to similar blast loads, and enhancing the blast resistant capacity substantially.
2. Investigation into the effect of axial loading on columns subjected to blasts has been performed and the results show that the axially loaded specimens have smaller deflections for UHPRC members. The axial loading changes the column boundary condition and limits the end rotation, and the influence from boundary change outweighs the P delta effect which results in a reduced mid span deflection.

Acknowledgements

The research presented in this paper jointly supported by The National Basic Research Programme 2015CB058002, and the Key Projects of Tianjin Science and Technology Support Plan 14ZCZDSF0016, and the ARC Discovery Grant DP140103025 and DP160104661, is gratefully acknowledged.

References

[1] Schenker A, Anteby I, Nizri E, Ostraich B, Kivity Y, Sadot O, et al. Foam-protected reinforced concrete structures under impact: experimental and numerical studies. J Struct Eng 2005;131(8):1233–42.
[2] Aydin S, Yazici H, Baradan B. High temperature resistance of normal strength and autoclaved high strength mortars incorporated polypropylene and steel fibers. Constr Build Mater 2008;22(4):504–12.
[3] Ng KW, Garder J, Sritharan S. Investigation of ultra high performance concrete piles for integral abutment bridges. Eng Struct 2015;105:220–30.
[4] Li J, Wu C, Hao H. Investigation of ultra-high performance concrete slab and normal strength concrete slab under contact explosion. Eng Struct 2015;102:395–408.
[5] Yoo DY, Yoon YS. Structural performance of ultra-high-performance concrete beams with different steel fibers. Eng Struct 2015;102:409–23.
[6] Michael S, Ekkehard F. Ultra-high-performance concrete: research, development and application in Europe. In: Proceeding of the 7th international symposium on the utilization of UHS/HPC; 2005. p. 51–77.
[7] Na-Hyun Y, Kim J-HJ, Han T-S, Cho Y-G, Lee JH. Blast-resistant characteristics of ultra-high strength concrete and reactive powder concrete. Constr Build Mater 2012;28:694–707.
[8] Ghani Razaqpur A, Tolba A, Contestabile E. Blast loading response of reinforced concrete panels reinforced with externally bonded GFRP laminates. Compos B Eng 2007;38:535–46.
[9] Brandt A. Fibre reinforced cement-based (FRC) composites after over 40 years of development in building and civil engineering. Compos Struct 2008;86(1):3–9.
[10] Kang ST, Lee Y, Park YD, Kim JK. Tensile fracture properties of an ultra high performance fiber reinforced concrete (UHPFRC) with steel fiber. Compos Struct 2010;92:61–71.
[11] Farnam Y, Mohammadi S, Shekarchi M. Experimental and numerical investigations of low velocity impact behavior of high-performance fiber-reinforced cement based composite. Int J Impact Eng 2010;37:220–9.
[12] Rong Z, Sun W, Zhang Y. Dynamic compression behavior of ultra-high performance cement based composite. Int J Impact Eng 2010;37:515–20.
[13] Yang IH, Joh C, Kim B-S. Structural behavior of ultra high performance concrete beams subjected to bending. Eng Struct 2010;32(11):3478–87.
[14] Mahmud GH, Yang Z, Hassan AMT. Experimental and numerical studies of size effects of ultra high performance steel fibre reinforced concrete (UHPFRC) beams. Constr Build Mater 2013;48:1027–34.

[15] Millard SG, Molyneaux TCK, Barnett SJ, Gao X. Dynamic enhancement of blast-resistant ultra high performance fibre-reinforced concrete under flexural and shear loading. Int J Impact Eng 2010;37(4):405–13.
[16] Máca P, Sovják R, Konvalinka P. Mix design of UHPFRC and its response to projectile impact. Int J Impact Eng 2014;63:158–63.
[17] Wu C, Oehlers DJ, Wahchl J, Glynn C, Spencer A, Merrigan M, Day I. Blast testing of RC slabs retrofitted with NSM CFRP plates. Adv Struct Eng 2007;10(4):397–414.
[18] Wu C, Huang L, Oehlers D. Blast testing of aluminum foam-protected reinforced concrete slabs. J Perform Constr Facil 2010;25(5):464–74.
[19] Williamson G. Response of fibrous-reinforced concrete to explosive loadings, Technical Report. Cincinnati, Ohio: Depart of the army Ohio River Division Laboratories, Corps of Engineers; 1966.
[20] Ngo T, Mendis P, Krauthammer T. Behavior of ultrahigh-strength prestressed concrete panels subjected to blast loading. J Struct Eng 2007;133(11):1582–90.
[21] Magnusson J. Fibre reinforced concrete beams subjected to air blast loading. Struct Mater 2004;15:53–62.
[22] Lok T, Xiao J. Steel–fibre-reinforced concrete panels exposed to air blast loading. Proc Inst Civ Eng: Struct Build 1999;134(4):319–31.
[23] Habel K, Gauvreau P. Response of ultra-high performance fiber reinforced concrete (UHPFRC) to impact and static loading. Cement Concr Compos 2008;30:938–46.
[24] Wu C, Oehlers D, Rebentrost M, Leach J, Whittaker A. Blast testing of ultra-high performance fibre and FRP-retrofitted concrete slabs. Eng Struct 2009;31:2060–9.
[25] Imbeau P. Response of reinforced concrete columns subjected to impact load. Ottawa, Canada: University of Ottawa; 2012.
[26] Elsanadedy H, Almusallam T, Abbas H, Al-Salloum Y, Alsayed S. Effect of blast loading on CFRP-Retrofitted RC columns-a numerical study. Latin Am J Solids Struct 2011;8:55–81.
[27] Bao X, Li B. Residual strength of blast damaged reinforced concrete columns. Int J Impact Eng 2010;37(3):295–308.
[28] Fujikake K, Aemlaor P. Damage of reinforced concrete columns under demolition blasting. Eng Struct 2013;55:116–25.
[29] Kishi N, Mikami H, Ando T. Impact-resistant behavior of shear-failure-type RC beams under falling-weight impact loading. In: Proceedings of the 7th international conference on structures under shock and impact; 2002. p. 499–508.
[30] Shi Y, Hao H, Li Z. Numerical derivation of pressure–impulse diagrams for prediction of RC column damage to blast loads. Int J Impact Eng 2008;35(11):1213–27.
[31] Crawford J, Malwar L, Morrill K. Reinforced concrete column retrofit methods for seismic and blast protection. In: Proc. of society of American military engineering symposium on compressive force protection, Charleston, USA; 2001.
[32] Imbeau P. Response of reinforced concrete columns subjected to impact loading. Ottawa, Canada: Department of Civil Engineering University of Ottawa; 2012.